

Article

In Situ Evaluation of New Silica Nanosystems as Long-Lasting Methods to Prevent Stone Monument Biodeterioration

Flavia Bartoli ^{1,2} , Zohreh Hosseini ^{2,*} , Valerio Graziani ³ , Martina Zuena ², Carlo Venettacci ¹, Giancarlo Della Ventura ² , Luca Tortora ³ , Armida Sodo ²  and Giulia Caneva ² 

¹ Institute of Heritage Science, National Research Council, ISPC-CNR, 00010 Rome, Italy; flavia.bartoli@cnr.it (F.B.); carlo.venettacci@uniroma3.it (C.V.)

² Department of Science, University of Roma Tre, 00146 Rome, Italy; martina.zuena@uniroma3.it (M.Z.); giancarlo.dellaventura@uniroma3.it (G.D.V.); armida.sodo@uniroma3.it (A.S.); giulia.caneva@uniroma3.it (G.C.)

³ Roma Tre Surface Analysis Laboratory, National Institute for Nuclear Physics, Department of Science, University of Roma Tre, 00146 Rome, Italy; valerio.graziani@roma3.infn.it (V.G.); luca.tortora@uniroma3.it (L.T.)

* Correspondence: seyedhzhohreh.hosseini@uniroma3.it

Abstract: Microbial colonization can lead to various biodeterioration phenomena in outdoor stone monuments. To prevent these issues and mitigate the negative effects of chemical control, recent research has focused on encapsulating biocides in nanostructures. We tested the antifouling efficiency of the new multifunctional coating through in situ experiments performed on the Aurelian Walls in Rome. We selected two different biocides (2-mercaptobenzothiazole and zosteric sodium salt) and loaded them into two different silica nanocontainers (nanocapsules and mesoporous particles), which were dispersed in TEOS coatings. These coatings were applied to four common lithotypes (marble, travertine, mortar, and brick). Subsequently, we accelerated the colonization by inoculating microorganisms onto half of the samples, subjecting all samples to aging cycles. We conducted colorimetric, infrared spectroscopy, and other microscopic analyses to assess their durability and antimicrobial action. Our 3-year survey indicates that the coatings demonstrated antifoulant efficiency across all samples, with higher effectiveness observed on brick and mortar compared to travertine and marble. Among the nanostructures, nanocapsules exhibited greater efficiency than mesoporous particles, and regarding the biocides, the commercial one outperformed the natural one. These findings highlighted the potential of such systems in preserving cultural heritage; however, further research and product development is imperative for practical implementation.

Keywords: Aurelian Walls; natural biocide; nanoencapsulation; biofilm; stone monument; weathering; coating TEOS; multifunctional coating



Citation: Bartoli, F.; Hosseini, Z.; Graziani, V.; Zuena, M.; Venettacci, C.; Della Ventura, G.; Tortora, L.; Sodo, A.; Caneva, G. In Situ Evaluation of New Silica Nanosystems as Long-Lasting Methods to Prevent Stone Monument Biodeterioration. *Coatings* **2024**, *14*, 163. <https://doi.org/10.3390/coatings14020163>

Academic Editor: Simona Liliana Iconaru

Received: 20 December 2023

Revised: 11 January 2024

Accepted: 24 January 2024

Published: 26 January 2024



Copyright: © 2024 by the authors. Licensee MDPI, Basel, Switzerland. This article is an open access article distributed under the terms and conditions of the Creative Commons Attribution (CC BY) license (<https://creativecommons.org/licenses/by/4.0/>).

1. Introduction

Biodeterioration of monuments in open-air environments is a complex process influenced by atmospheric and edaphic conditions, including potential microorganism occurrences [1–7]. In particular, the growth and metabolic activity of algae, cyanobacteria, and lichens, as well as mosses and higher plants, can lead to various forms of biodeterioration through biochemical activities and biogeochemical cycles [5,8–15]. Microbial colonization of stones is regulated by natural parameters such as light and moisture [16–18]. It typically commences with phototrophic organisms that build up a visible protective biofilm enriched with inorganic and organic biomass on the nutrient-depleted stone surface [19].

For heritage conservation and biodeterioration management, various control methods, which are categorized as physical, mechanical, and biochemical approaches, have been utilized [20–25]. Biocides, among these methods, are more commonly employed to eliminate or prevent the formation of organism biofilms [26–28]. However, biocide application

cannot have a long-lasting efficiency, and repetitive use may result in microbial resistance, leading to a resurgence of microbes on treated surfaces [23,29,30]. Moreover, their potential risks to human health and the environment, as well as substrate interference [31,32], have prompted a quest for alternative ecofriendly solutions [33–35].

In recent years, extensive research has focused on the development of natural biocides and innovative materials in controlling the biodeterioration of stone monuments [36–42]. Natural biocides derived from plant extracts or essential oils usually provide an environmentally friendly alternative to traditional chemical biocides, often reducing the impact on both cultural artifacts and the surrounding environment [34,38,42–48]. Some substances have been tested for their efficacy against various biodeteriogens, including bacteria, fungi, cyanobacteria, and algae [49–52].

Furthermore, one technological advancement is the encapsulation of natural biocides in various nanostructures, such as silica nanoparticles or nanocapsules, for long-lasting reliability and selective activity [53–57]. These nanosystems offer controlled release mechanisms and provide an ecofriendly and sustainable approach to preserving cultural heritage [54]. They provide controlled delivery systems ensuring a prolonged and targeted release of the biocidal agents, thereby enhancing their efficiency [58–60]. By employing nanotechnologies, lower quantities of biocides are required, minimizing their environmental footprint while maintaining their effectiveness in combating microbial colonization on historical monuments [54,56,60,61]. This integrated approach not only ensures the preservation of valuable cultural heritage but also contributes to sustainable practices and long-term protection [62–64].

In the context of two scientific projects for the conservation of cultural heritage (SUPERARE and GRAL: Progetti Gruppi di Ricerca 2020, Regione Lazio), several laboratory tests have been conducted. The first step was aimed at defining the synthesis and characterizing the silica nanosystems, such as nanocapsules (NC) and mesoporous nanoparticles (MNP) loaded through the encapsulation step with biocides like 2-mercaptobenzothiazole (MBT) and zosteric sodium salt (ZOS) [55,56]. Later, Bartoli et al. [60], through several *in vitro* analyses, evaluated the antimicrobial efficiency of two MBT and ZOS biocidal agents loaded in silica nanosystems, demonstrating their promising antifouling and antimicrobial properties. All these findings represent a significant step in the development of new ecofriendly and sustainable technologies for cultural heritage conservation. While *in vitro* tests provide controlled laboratory conditions to evaluate the potential efficacy of treatments to prevent biological colonization, *in situ* tests are essential for assessing the long-term impact of these methods in real environmental settings. Therefore, in the context of these projects, the aim of the present contribution is the performance of *in situ* tests to evaluate the efficiency of new multifunctional coatings containing different nanosystems loaded with natural and commercial biocides. Through a pluriennial evaluation of more than 3 years, we will evaluate their durability over time and antimicrobial long-term effectiveness to prevent the colonization of biodeteriogens.

2. Materials and Methods

2.1. Biocide, Lithotypes, and Coatings

2.1.1. Biocide and Their Nanocontainers

We selected two different biocides, based on the previous work of Ruggiero et al. [40–42,51], namely 2-mercaptobenzothiazole (MBT) and zosteric sodium salt (ZOS). ZOS is a natural antifouling product derived from *Zostera marina* L. [47,65–69], while MBT is a commercial biocide widely used in the treatment of cultural heritage [70]. As reported in Ruggiero et al. [55], we synthesized ZOS from *trans*-4-hydroxycinnamic and the sulfur trioxide pyridine complex. Additionally, according to Ruggiero et al. [55,56], we synthesized two different silica nanocontainers, namely core–shell nanocapsules (NC) and mesoporous nanoparticles (MNP).

2.1.2. Lithotypes Selection and Aging

To verify the long-term efficacy of the nanostructured coatings, we selected four lithotypes commonly found in artworks and monuments: Carrara marble, travertine, mortar, and brick. All the samples, sized $5 \times 5 \times 1$ cm, were prepared by a specialized group of restorers (CBC, Rome, Italy). Red-fired bricks (MT) were purchased from a local company (the CBC *Conservazione Beni Culturali*, Rome, Italy). Travertine (TR) and Carrara marble (MR) were purchased directly from quarries in Tivoli and Carrara, respectively. The lime-based mortar (ML) was prepared by using natural hydraulic lime (NHL 5) provided by Saint Astier (the CBC *Conservazione Beni Culturali*, Rome, Italy) and mixed with standard river sand aggregates (size < 4 mm) in a 1:2 proportion, adding water to achieve good workability. The mortar mixture was cured for 24 h at room conditions (RH% = 50%, 20 °C) and used for experiments after 28 days [71].

Travertine and Carrara marble samples underwent an accelerated artificial aging process to increase their porosity and facilitate the coating absorption: two heating cycles at 600 °C and subsequent overnight immersion in water at room temperature, following the standard set by the American Society for Testing and Materials International [71,72].

2.1.3. Coating Development and Aging

The nanoparticles were dispersed in a coating using tetraethyl orthosilicate (TEOS), ethanol (Carlo Erba Reagents S.r.l., Cornaredo, Italy), poly (dimethylsiloxane) hydroxyl-terminated (PDMS-OH, Sigma-Aldrich, St. Louis, MO, USA), and n-octylamine (Sigma-Aldrich, St. Louis, MO, USA) as a nonionic surfactant, without further purification following Normal 43/93 [73]. This process followed the protocol previously outlined by Zuenaga et al. [71,74].

To stimulate a potential real application procedure on monuments, the coatings were applied by a brush until saturation, ensuring the stone surface remained wet for more than 1 min. For bricks and mortars, a total of 16 brushes were required, while after aging, 4 brushes were needed for travertine and 6 for Carrara marble due to their different porosity and subsequent absorption rate [71,74]. Approximately one week was necessary for the coating to solidify through polymerization and water evaporation, during which time the samples were kept under laboratory conditions (RH% = 50%, 20 °C) [71,74].

To verify the durability of the coating (inalterability and chemical resistance), we conducted artificial aging. Initially, the aging conditions were based on the technical standards outlined in the American Society for Testing and Materials International ASTM D4303-10 [75]. We employed artificial UV aging in an ACS climatic chamber equipped with a 125W Hg UV lamp, emitting 200 W/m² irradiance and continuous exposure for 360 h (15 days). Throughout our study, we implemented two aging cycles: The first one simulated the most plausible natural environmental conditions (with a temperature of 30 °C and 50% relative humidity—RH). The second one stimulated more stressful conditions, approaching the limits of those usually occurring in the natural environment (with a temperature of 40 °C and 60% RH).

To evaluate the changes in the coating after aging, we performed colorimetric analysis and Fourier transform infrared spectroscopy (FTIR). Colorimetric measurements were performed according to the procedure described in the European Standard (UNI-EN 15886) [76]; Uni Normal 43/93 [73]. We preliminarily observed and investigated the physical properties of the 4 selected lithotypes after the application of the different coating formulations (a total of 90 samples). Following the most used interference tests [32], we specifically examined whether these products induced alterations in the surface optical properties that might result in a noticeable color change (measured by ΔE) perceivable to the human eye, potentially affecting the perception variation in hypothetically treated artifacts. Colorimetric measurements were carried out on three different points for each sample, and average values of L^* , a^* , and b^* were obtained for each sample group (untreated, coating only, and the two systems of nanosystems with the two tested biocides: NC-MBT, MNP-MBT, NC-ZOS, and MNP-ZOS). The uncertainty associated with ΔE_{aging}

was determined as the standard deviation of the average value concerning the white reference. In the spectroscopic analyses, a Thermo Scientific Nicolet iS50 FTIR (Thermo Fisher Scientific, Madison, WI, USA) spectrometer was employed, with two experimental approaches: attenuated Total Reflectance (ATR) and μ -ATR mode. Spectra were collected in the 4000–400 cm^{-1} range with 4 cm^{-1} nominal resolution, averaging 64 scans for both sample and background. M-ATR mode was chosen to enhance the sample surface response while lowering as low as possible the bulk contribution. The measurements were carried out by using the Thermo Scientific Nicolet Continuum FTIR microscope equipped with a liquid-nitrogen-cooled mercury–cadmium–telluride (MCT) detector and a germanium crystal. The spectral range was 4000–650 cm^{-1} with 8 cm^{-1} nominal resolution; final spectra were obtained by averaging 64 scans.

2.2. In Situ Tests

To characterize the biocidal efficacy of coatings in the outdoor environment, we selected the northward-facing section of the Aurelian Walls near Porta San Sebastiano in Rome as our experimental site (Figure 1a). We tested ten different conditions for each lithotype, resulting in a total of 40 samples: (8) without any treatment and (32) by combining the nanosystems (NC and MNP) with the biocide (MBT and ZOS) and with or without a biological culture (inoculum and no inoculum) (2 nanosystems \times 2 biocides \times 2 possible conditions of inoculum \times 4 lithotypes) to stress the coating efficiency in fighting the biological colonization (Table 1). For the inoculum materials, the biological patinas collected in situ during the experiments were cultivated using a BG-11 and BBM liquid media (Sigma-Aldrich) at 25 °C under natural sunlight conditions, following the methodology detailed by Bartoli et al. [60]. Additionally, to identify the microorganisms composing the biological community's growth in the culture media after its plating on Petri dishes, we conducted a morphological analysis under an optical microscope, as reported by Bartoli et al. [60]. Before the outdoor exposure, we inoculated 2 mL of culture on the 20 samples, waiting for the culture stabilization. After two weeks in February 2020, we exposed all 40 samples in situ on the Aurelian Walls, conducting monthly evaluations for three years until May 2023.

Table 1. Scheme of composition of the tested samples for each lithotype.

Coating Composition			
No Inoculum		Inoculum *	
Biocide	Samples	Biocide	Samples *
Untreated	A	Untreated	B *
MBT	NC	MBT	NC *
ZOS	NC	ZOS	NC *
MBT	MNP	MBT	MNP *
ZOS	MNP	ZOS	MNP *

The * is related to the inoculum phase.

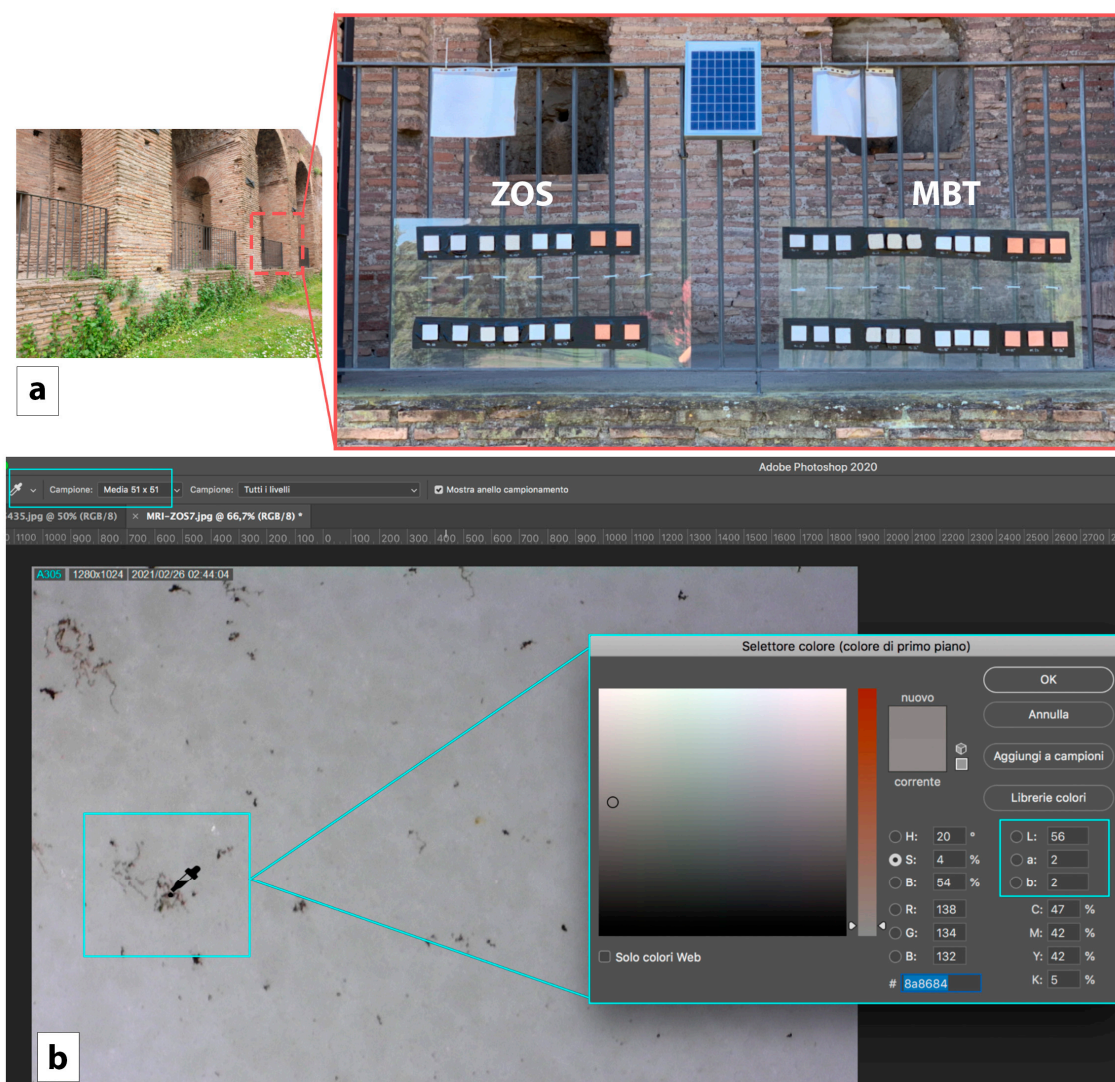


Figure 1. Sampling site (a) and colorimetric analysis method (b). MBT: 2-mercaptobenzothiazole, ZOS: zosteric sodium salt.

2.2.1. Microscopic and Colorimetric Analysis

We monitored monthly the effectiveness of the experimental biocides against colonization of the microorganisms using UV/VIS light microscopy techniques. For this purpose, a Dino-Lite nonpolarized visible-light digital microscope was used to investigate the samples at $60\times$ and $220\times$ magnifications. We captured four photos of four distinct parts of tiles under both VIS and UV lights for each sample. Subsequently, a detailed analysis was carried out using a Hirox digital stereoscope (Hirox RX 100, HIROX EUROPE, Limonest, France, lens 2500, magnification $1500\times$, multifocal 3D final image) to identify the biological colonization developed on the different tiles throughout their exposure to the environmental conditions.

Then, we performed an image analysis using the Photoshop (PsD6, 2022) program to quantify the colonization rate and evaluate the effectiveness of different treatments. We applied the eyedropper functionality within the software, which corresponds to the L^* , a^* , and b^* color values according to the methodology outlined by Bartoli et al. [77] (Figure 1b). For each optical image, we selected 10 random test areas mounting to 40 test areas for each individual tile under investigation. We set the eyedropper sampler at an average of 51×51 pixels to cover an area of approximately 2601 pixels for each measurement, ensuring comprehensive coverage across the samples.

Along with lightness measurements (L^*), based on colorimetric variations to darkening of the surfaces due to light exposure, to evaluate the biological colonization for each tile, we calculated the variation of $\Delta L_{2023-2020}$ as a function of the experiment time. Moreover, we calculated $\Delta L_{2020}^{\text{Treated-noTreated}}$ and $\Delta L_{2023}^{\text{Treated-noTreated}}$ to derive the difference between the samples with a multifunctional coating (treated) and those without any treatment (untreated) during the exposure time ($\Delta L_{2023-2020}^{\text{Treated-noTreated}}$).

2.2.2. Microclimate Evaluation

The microclimate of the sampling site was evaluated using an environmental monitoring system (EMS) specifically designed for this project. The system was solar-powered and capable of internet connectivity for remote monitoring. The EMS was based on an Arduino UNO Rev.3 microcontroller due to its ease of power supply, low power consumption, sufficient pin availability, and compatibility with sensors used in the setup. Temperature and relative humidity (RH) were continuously monitored via an FS200-SHT20 i2C sensor having high repeatability ($\pm 0.1\%$ on both RH and T, according to the manufacturer). The internet connection was assured via a dedicated SIM card, and the ThingSpeak platform (<https://thingspeak.com>) was employed for data storage, visualization, and manipulation, offering customizable displays, geolocation features, and system status updates. Data were collected from July 2021 to October 2023.

3. Results

3.1. Coating Tests

3.1.1. Comparison between Pretreating and After-Treating Samples

Figure 2 shows the $\Delta E_{\text{Treatment}}$ calculated on the difference between the group values of L^* , a^* , and b^* for each treatment (i.e., different coating applications) and the untreated ones. $\Delta E_{\text{Treatment}}$ is expected to be below the threshold value for eye sensitivity ($\Delta E_{\text{Threshold}} = 4$). Dissimilarities in the infrared spectra among the different formulations of the coating are not expected.

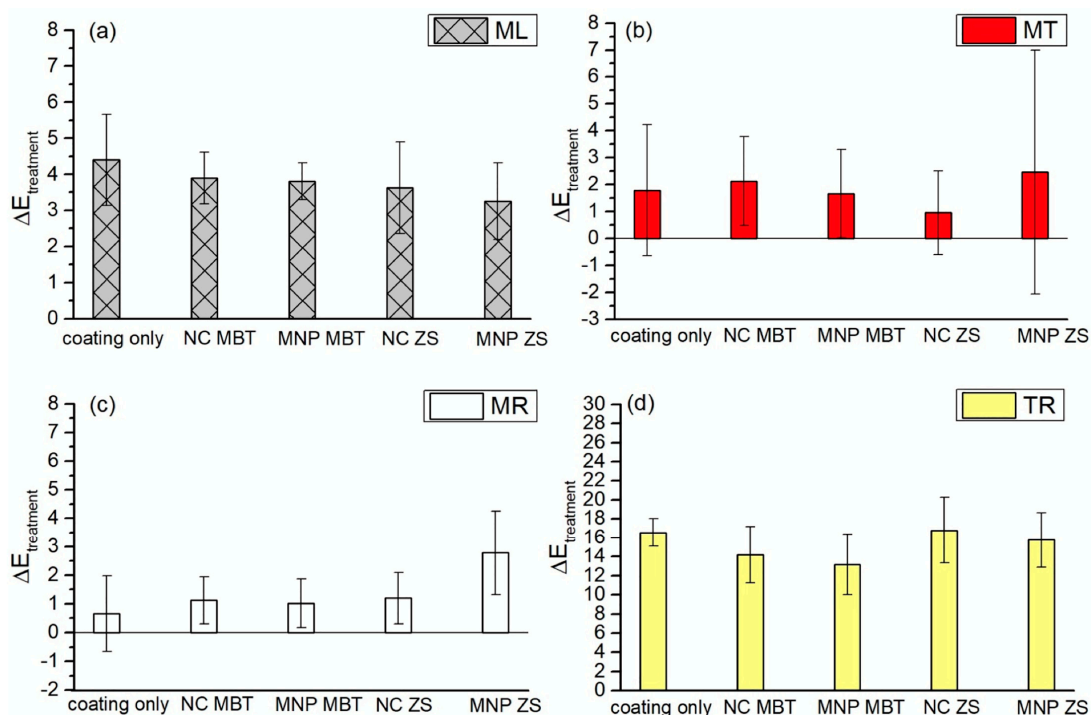


Figure 2. Color variation in treatment groups after coating treatment: (a) mortar (ML); (b) brick (MT); (c) Carrara marble (MR); (d) travertine (TR).

Figure 2a–c show that for mortar, brick, and Carrara marble, none of the treatments demonstrated a color change perceptible to the human eye (Student's *t*-test probabilities greater than the critical value of 0.05 for these lithotypes). For all these materials, the recorded values are mostly below $\Delta E_{\text{Treatment}} = 4$, even considering uncertainty intervals, indicating minimal color variations. Notably, mortars exhibited the most substantial average variation. Conversely, travertine showed wide variations with an average value $\Delta E_{\text{Treatment}} = 15 \pm 2$ (Figure 2d) that can be mostly explained by the difference in ΔL^* ($\Delta L^*/\Delta E_{\text{Treatment}} > 0.99\%$ for all treatments carried out for this material). Because of the natural, random variability of the variety of stones used in this study, there is a color difference between pristine samples used for the untreated group and those used for the treated group.

3.1.2. Comparison between Pre-Aging and After-Aging Samples

The colorimetric measurements and spectroscopic comparisons between unaged and aged specimens demonstrated good durability and stability of the coatings applied. No statistically significant color differences were found for any of the investigated materials (Figure 3a).

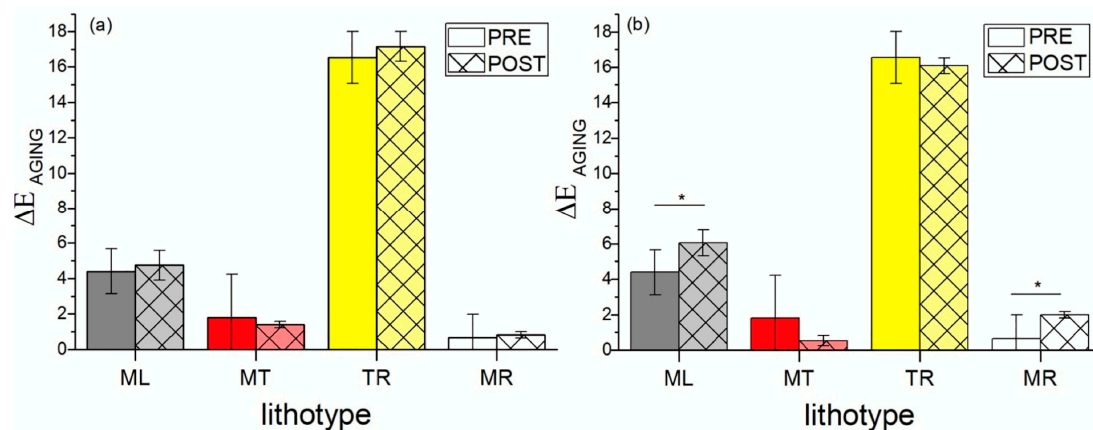


Figure 3. (a) Color variation in coating-only-treated samples for the 4 lithotypes after the first aging cycle; (b) color variation in coating-only-treated samples for the 4 lithotypes after the second aging cycle; * = student's *t* $p < 0.05$. PRE stands for pretreatment samples, and POST stands for post-treatment samples.

Figure 3b shows a comparison between pre-aging and post-aging ΔE values for the four lithotypes following the second accelerated aging cycle (values are referred to as the white standard). In this instance, the first small but significant color variations, albeit minimal, were observed for the mortar and Carrara marble samples. In both cases, the difference was attributed to a slight increase in the b^* values, indicating a yellowing effect in these materials.

Unlike the previous aging cycle, μ -ATR analyses were performed on the Carrara marble samples to further investigate this evidence. The analyses confirmed a general overlap between the pre-aging and post-aging spectra for all materials, as depicted in Figure 3b. Therefore, the color variation must be attributed to a component present below the detection limit of the technique.

3.2. In Situ Tests

3.2.1. Microclimate

The microclimatic data logger, installed to monitor the temperature and the relative humidity conditions, showed the maximum temperatures (25–30 °C) during the summer (from May to September) and the lowest temperatures (5–14 °C) during winter (from

December to March) (Figure 4) The relative humidity data reflects a humid condition with a variance between 40% RH in the hot months to 90% RH in the cold months.

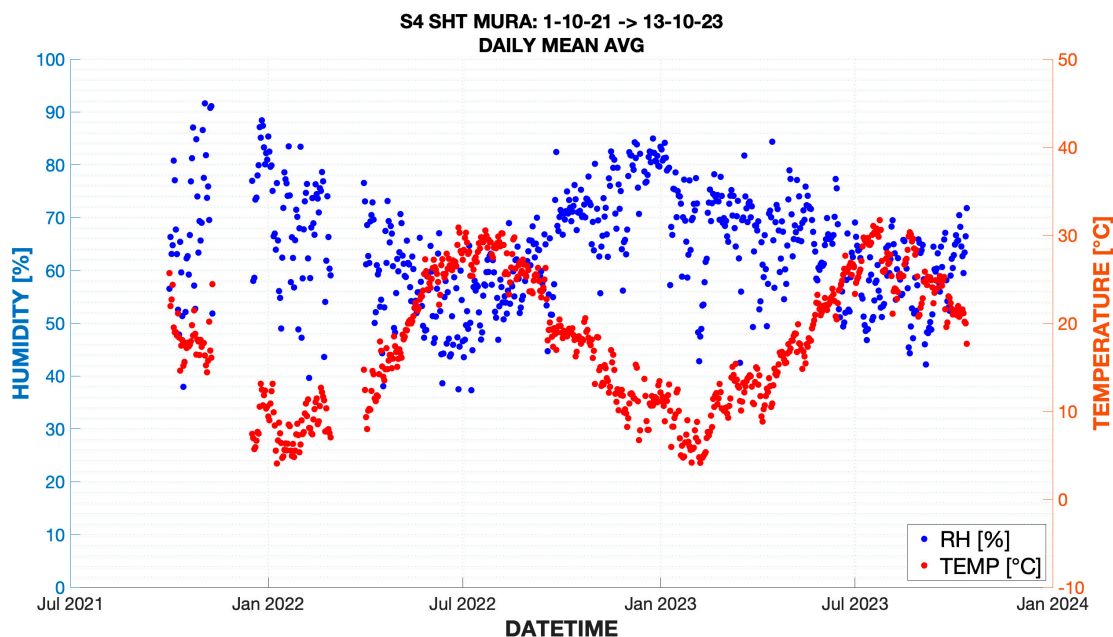


Figure 4. Microclimatic conditions on the Aurelian Walls (Rome) from July 2021 to October 2023. Daily average values of temperature (°C in red) and of relative humidity (RH% in blue).

3.2.2. Biocidal Efficiency

The macroscopic and microscopic monitoring of the samples over time revealed significant differences. When assessing color changes associated with the colonization rate, we observed the emergence of black spots on the surfaces at times. In some cases, especially for the non-inoculated samples, minimal colonization resulted in color variation below the threshold of human eye sensitivity. Conversely, the acceleration induced on the inoculated samples highlighted the efficiency rate of the coatings, resulting in a color variation that exceeded the threshold of human eye sensitivity. Indeed, the variation of ΔE became noticeable to the human eye when samples that initially appeared green, due to the inoculation of communities mainly composed of algae and cyanobacteria (Figure 5a), transitioned to colonization mainly by black meristematic fungi (Figure 5b), which form black spot visible on the stone surface.

Moreover, during the inoculum, we observed varying degrees of waterproofing among the different coatings (Figure 6c), showing a decreasing trend from mortar and brick to marble and travertine.

The variation in lightness ($\Delta L_{2023-2020}$) of the not-inoculated samples remained minimal for the untreated samples (A) across all lithotypes and for the main treated samples (Figure 5a), with values below the unit. Only samples of Carrara marble and travertine showed a higher ΔL , demonstrating a certain colonization rate (Figure S1).

The comparison of $\Delta L_{2023-2020}^{\text{Treated-noTreated}}$ at the end of the testing period revealed a partial progression of colonization in the case of Carrara marble and travertine samples, showing slight differences among the testing conditions (biocides and nanosystems). In both lithotypes, we noted a higher efficiency of the commercial biocide (MBT) compared to the natural one (ZOS) under the testing conditions. For the nanosystems, the efficiency varied based on lithotypes and biocides (Figure 6b). However, the multifunctional coating on mortar and brick did not display a clear efficiency rate, probably due to the low colonization trend for an accurate quantitative evaluation. The ΔL was influenced by the high heterogeneity of the surface (Figure S2).

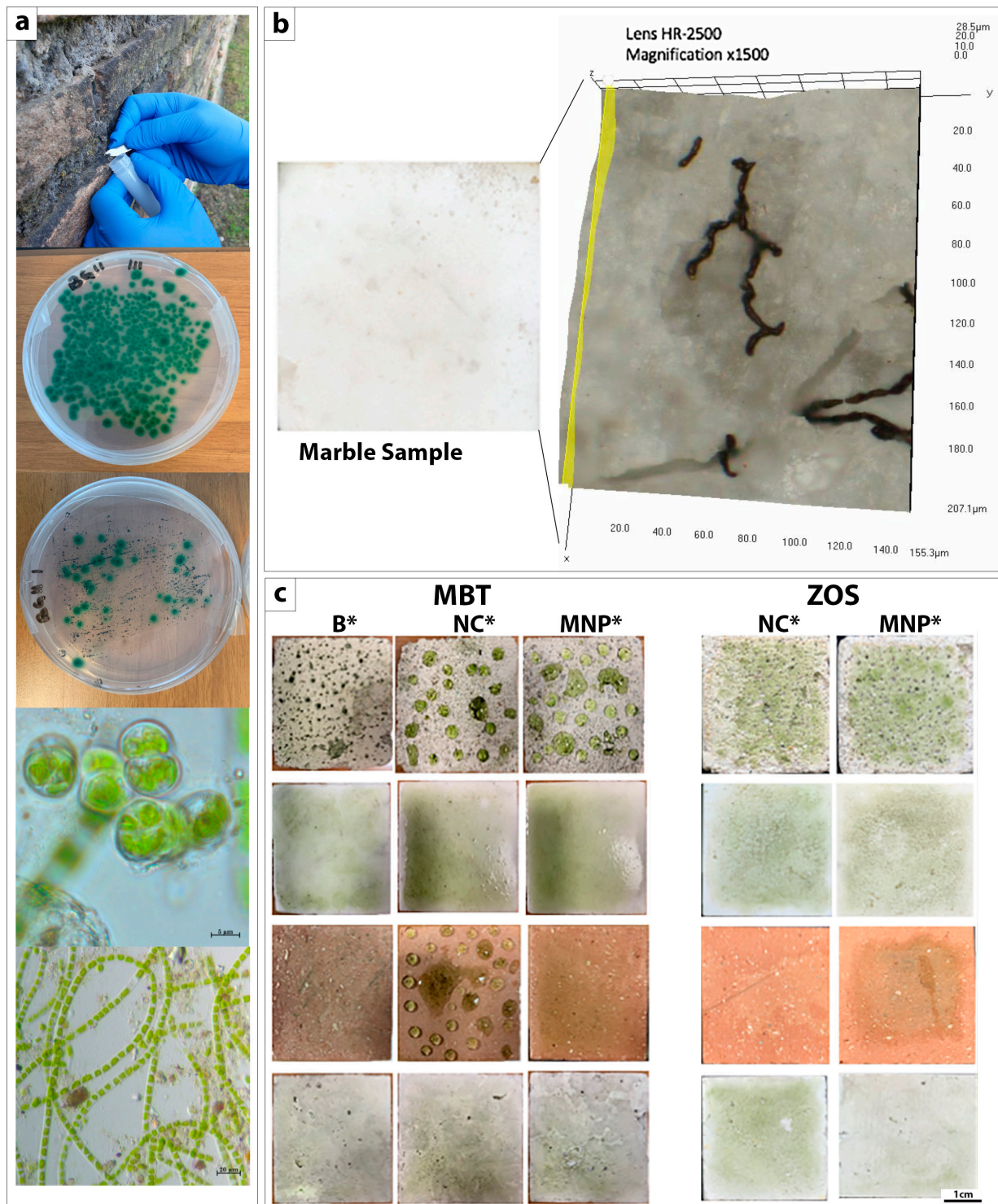


Figure 5. Inoculum phase. (a) Collection of biological samples in situ, culture by plating and optical microscopic observation to morphological identification of green algae and cyanobacteria; (b) 3D image of final colonization on all samples by Hirox stereoscope due to meristematic fungi; (c) lithotype and coating behavior during inoculum application. MBT (2-mercaptobenzothiazole), ZOS (zosteric sodium salt), ML (Mortar), MR (Carrara Marble), MT (Brick), TRI (Travertine), B* (Untreated), NC* (core-shell nanocapsules), and MNP* (mesoporous nanoparticles). The * is related to the inoculum phase.

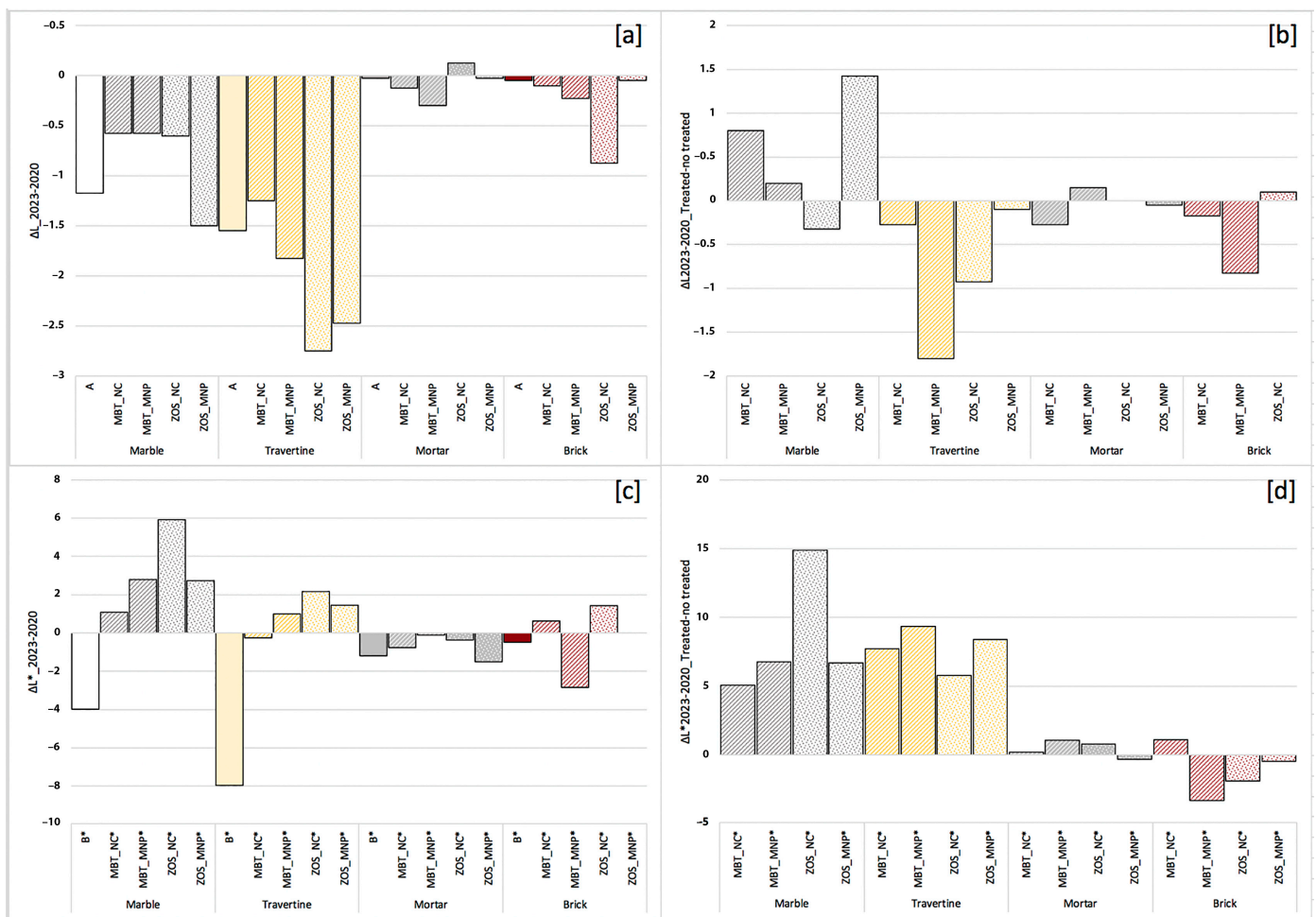


Figure 6. Lightness variation as a function of time ($\Delta L_{2023-2020}$) and ΔL rate between treated and nontreated samples ($\Delta L_{2023-2020}^{\text{Treated-noTreated}}$), respectively, for non-inoculated (a,b) and inoculated (c,d) samples. The * is related to the inoculum phase.

The darkening ($\Delta L^*_{2023-2020}$) of all untreated substrates was evident (Figure 6c). Particularly, for Carrara marble and travertine, the darkening rate in the untreated samples was notable, as well as the brightening rate in the treated samples. For mortar and bricks, the observation was less distinct but still discernible in certain instances.

When evaluating the lightness variation between treated and untreated samples ($\Delta L_{2023-2020}^{\text{Treated-noTreated}}$), the supplementary inoculum application revealed a higher visible efficiency of the treatment for Carrara marble and travertine, while a lower efficiency was observed for mortar and brick (Figure 6d).

4. Discussion

In this study, we conducted in situ experiments to test several variables aiming to evaluate the efficiency of different multifunctional coatings.

The comparison among the various coatings within the same lithotype group confirmed that the coatings had a similar impact on color, resulting in an overall low impact on the perception of the human eye. This effect resulted not only from the efficacy of the nanoscaled particle dispersion in preventing light scattering but also from the overall low viscosity achieved by the products [78]. This characteristic facilitated the application of extremely thin, nonfilm-forming coatings capable of penetrating the porosity of the materials (which were significantly present in all samples except for Carrara marble) [71,74,79].

All coatings showed similar behavior, suggesting that the different particles and their contents did not significantly contribute to any chromatic interference at that stage, which is

consistent with previous data [74,80,81]. Previous results have demonstrated that following treatment, all surfaces acquired waterproof properties, resulting in a substantial reduction in the capillary water absorption coefficient. In addition, the natural water vapor transmission rate behavior of the stones was not significantly affected. The coatings appeared uniformly distributed on the stone surfaces and did not cause optical variations visible to the naked eye. Furthermore, the presence of TiO₂ nanoparticles and silica nanocontainers did not alter the optical appearance of the stones. Optical surface roughness (OSR) and SEM analyses revealed no changes in roughness and confirmed that all coatings were homogenous and free from cracks. SEM–EDS analysis showed a homogenous distribution of both Ti and Si on the surface of all treated stones. The cross-sections verified that the coatings remained at the surfaces, serving a protective function [71,74].

The aging test did not show statistically significant color differences for any of the investigated materials. Only after the second accelerated aging cycle was a significant variation detected, demonstrating good durability and stability of the coating. A possible hypothesis for the observed yellowing of the material after the aging phase could be the oxidation of iron impurities present in the specific quality of marble used in this study, possibly favored by the combined presence of high humidity and UV radiation [82,83]. Moreover, variations in mineral composition and surface characteristics within different types of marble and travertine can also influence the appearance of coatings. Some varieties might exhibit slight color alterations or differences in glossiness upon coating application, although these variations are often less prominent than those observed on more porous surfaces like mortar [71,72]. The concentration of these mineral impurities might reasonably be below the detection limit of the technique and, therefore, undetectable. This hypothesis also applies to the mortar samples, as the sand might contain iron-releasing minerals.

The aging conditions were designed to stimulate possible natural conditions in the outdoor environment, as confirmed by microclimatic data. The temperature and relative humidity values employed for the first accelerated aging cycle in the climatic chamber correspond to those observed during the monitored experiment period. For the second aging cycle, the temperature of 40 °C significantly exceeds the highest recorded value in the hottest month (August), while the choice of a higher relative humidity value, even though it typically decreases during the same period, serves as an intentional stressing factor. Then, our results provide predictive insights into the potential long-term durability of these coatings based on the stressed conditions applied during the aging cycles.

Additionally, the microclimatic data highlighted the favorable conditions for biological growth. Extensive evidence demonstrated that the initial stone colonization by microorganisms, especially cyanobacteria and green algae, is promoted by environmental conditions, notably water availability [14,84–88]. Similarly, prior studies into the new multifunctional coating have indicated a reduction in its efficiency under highly humid conditions [55,71,74]. In this work, we intentionally highly stressed the new silica nanosystems to assess their efficiency, choosing a site with a high humidity level and creating conditions that favor the growth of biodeteriogens.

Moreover, the capillary water absorption coefficient (CWAC) of tested lithotypes, closely related to their porosity, stands as a significant factor influencing microbial colonization [15,17,88,89]. Generally, mortar and travertine tend to have higher porosity and capillary water absorption coefficients compared to Carrara marble and brick, making them more susceptible to microbial colonization. In our study, brick and mortar exhibited a reduction in CWAC by over 95% following the coating application. In contrast, aged travertine and Carrara marble tiles displayed a lower reduction. This disparity could be attributed to the size ratio between nanoparticles and stone porosity. This disparity could be attributed to the size ratio between nanoparticles and stone porosity [71,74]. In fact, previous studies have indicated that nanoparticle presence enhances stone hydro-repellence, with a significant reduction in the water absorption rate in materials treated with TEOS-based coating, particularly evident in mortar and brick [71,74,90,91]. However,

the varying efficacy of antimicrobial coatings across these materials, due to their inherent porosity, poses challenges in achieving consistency and comprehensive protection.

A previous multitemporal study investigating the dynamics of recolonization by cyanobacterial populations on travertine in the Tiber River embankments [77] demonstrated that within the initial 3 years, no evident visual changes were observed. However, in the subsequent 1–2 years, a complete regrowth was detected. In this way, to simulate such recolonization phenomena within our experimental period, we induced the inoculum phase. This phase stressed the coating systems and highlighted their effectiveness in reducing the colonization process in all the tested lithotypes. Moreover, in outdoor artworks, the natural stone recolonization presents a certain variability, even within similar exposure and inclination of test areas, due to the difference in stone porosity and subsequent rainfall quantities [7,77,92]. For instance, the Tiber River embankments in Rome, constructed using similar travertine sourced from the Tivoli quarry [5,77], highlighted the significance of porosity in fostering microbial colonization. This relevance primarily stems from differential water absorption and retention due to varying porosity levels.

The relevant influence of water input in conditioning biological colonization was widely observed [93,94]. Usually, water content seems to be the primary conditioning factor among microclimatic factors influencing biological colonization; indeed, sites that are protected from rainfall, as well as incident water input or percolation, are free from biological colonization or exhibit minimal biological, even when other environmental conditions are favorable [93–96]. Consequently, water emerges as a limiting factor that governs the presence of mixed communities, aligning with Liebig and Shelford's ecological principles [97].

Then, the lower CWAC reduction observed in aged travertine and Carrara marble indicates a higher water availability, resulting in a greater colonization rate compared to brick and mortar. Consequently, changes in water input linked to the preservation treatments can create preferential growth conditions for specific species within the community [95,96]. This change might explain the dominance of meristematic fungi over the photosynthetic microorganisms, typically dominant in inoculated communities and generally found in the biopatinas on the Aurelian Walls, possibly due to the waterproofing effect of the applied coating. While the commercial biocide (MBT) exhibited superior efficacy compared to the natural biocide (ZOS), it is noteworthy that the ZOS also demonstrated a significant level of effectiveness. Previous studies have highlighted its potential when encapsulated within silica nanocapsules for controlled release in antifouling coatings [55]. Moreover, research by [47,66,67,69,98] identified *Zostera detritus* as a possible source of zosteric acid, the active component of this biocide. Further reinforcing its effectiveness [99] confirmed ZOS's capability to reduce bacterial attachment on coatings, suggesting its prowess as an antifoulant. These collective findings underscore the considerable potential of zosteric sodium salt as a natural and efficacious biocide. Despite its initial lower efficacy compared to MBT, the inherent potential of ZOS suggests the viability of optimizing its effectiveness by increasing its concentration within nanosystem formulations. Furthermore, the use of nanoencapsulation allows such a low quantity of biocide that even the utilization of commercial biocides could still be considered, minimizing their environmental toxicity. However, despite these promising initial results for this new formulation, it is important to note that longer-term studies would be necessary to simulate natural colonization on various lithotypes, demonstrating prolonged, slow-term control.

5. Conclusions

Silica nanosystems offer a promising technology for preserving cultural heritage due to their long-lasting reliability, enabling the controlled release of biocides and an ecofriendly approach. This nanotechnology reduces the quantity of biocides while enhancing the treatment effectiveness in preventing colonization. Indeed, our preliminary in situ experiments suggest that this treatment holds promise for preventive action on the colonization of stone monuments by biodeteriogens.

Our research demonstrates that the selected commercial biocide exhibits greater efficiency than the natural biocide, while the nanosystem minimizes its environmental impact, maintaining effectiveness through controlled release mechanisms. Furthermore, efficiency appears to be related to the lithotype, with nanocapsules showing greater effectiveness than mesoporous particles. However, our experiment, spanning 3 years of exposure, has limitations in assessing the long-term effectiveness and stability of these products. The inoculation phase and artificial aging of specimens imposed constraints; although promising, longer-term analysis on naturally aged stones is crucial for a more realistic comparison and control. Further research is necessary to identify the most efficient combination of biocide-nanosystems, pivotal for their effectiveness due to the release mechanisms.

Supplementary Materials: The following supporting information can be downloaded at: <https://www.mdpi.com/article/10.3390/coatings14020163/s1>, Figure S1: Optical image of Dino-lite digital microscope for each non-inoculated tile in 2020 and 2023; Figure S2: Optical image of Dino-lite digital microscope for each inoculated tile in 2020 and 2023.

Author Contributions: Conceptualization, F.B., M.Z., G.C., A.S. and G.D.V.; methodology, F.B., M.Z., V.G., G.C., A.S. and L.T.; software, F.B., M.Z., Z.H., V.G. and C.V.; validation, F.B., M.Z., Z.H., V.G., G.C., A.S., L.T. and G.D.V.; formal analysis, F.B., M.Z., Z.H., V.G. and C.V.; investigation, F.B., M.Z., Z.H., V.G. and C.V.; resources, G.C., A.S., L.T. and G.D.V.; writing—original draft preparation, F.B., Z.H. and V.G.; writing—review and editing, F.B., Z.H., V.G., C.V., G.C., A.S., L.T. and G.D.V.; visualization, G.C., A.S., L.T. and G.D.V.; supervision, G.C., A.S., L.T. and G.D.V.; project administration, G.C., A.S., L.T. and G.D.V.; funding acquisition, G.C., A.S., L.T. and G.D.V. All authors have read and agreed to the published version of the manuscript.

Funding: This research was funded by Regione Lazio, Italy, within the “GRAL—Green and Long—lasting stone conservation products” project (n. F85F21001710009) financed in the call “Progetto Gruppi di Ricerca 2020”.

Institutional Review Board Statement: Not applicable.

Informed Consent Statement: Informed consent was obtained from all subjects involved in the study.

Data Availability Statement: Data are contained within the article.

Acknowledgments: We thank the Capitoline Superintendence of Cultural Heritage for their collaboration and availability to access and carry out the experimentation in situ directly. We also thank the CBC *Conservazione Beni Culturali* for their cooperation in the preparation and supply of the samples for the study.

Conflicts of Interest: The authors declare no conflicts of interest.

References

- Herrera, L.K.; Videla, H.A. The importance of atmospheric effects on biodeterioration of cultural heritage constructional materials. *Int. Biodeterior. Biodegrad.* **2004**, *54*, 125–134. [[CrossRef](#)]
- Nuhoglu, Y.; Oguz, E.; Uslu, H.; Ozbek, A.; Ipekoglu, B.; Ocak, I.; Hasenekoglu, I. The accelerating effects of the microorganisms on biodeterioration of stone monuments under air pollution and continental-cold climatic conditions in Erzurum, Turkey. *Sci. Total Environ.* **2006**, *364*, 272–283. [[CrossRef](#)]
- Scheerer, S.; Ortega-Morales, O.; Gaylarde, C. Microbial deterioration of stone monuments—An updated overview. *Adv. Appl. Microbiol.* **2009**, *66*, 97–139. [[CrossRef](#)] [[PubMed](#)]
- Austigard, M.S.; Mattsson, J. Monitoring climate change related biodeterioration of protected historic buildings. *Int. J. Build. Pathol. Adapt.* **2019**, *38*, 529–538. [[CrossRef](#)]
- Caneva, G.; Nugari, M.P.; Salvadori, O. *Plant Biology for Cultural Heritage: Biodeterioration and Conservation*; The Getty Conservation Institute: Los Angeles, CA, USA, 2008.
- Liu, X.; Koestler, R.J.; Warscheid, T.; Katayama, Y.; Gu, J.D. Microbial deterioration and sustainable conservation of stone monuments and buildings. *Nat. Sustain.* **2020**, *3*, 991–1004. [[CrossRef](#)]
- Negi, A.; Sarethy, I.P. Microbial biodeterioration of cultural heritage: Events, colonization, and analyses. *Microb. Ecol.* **2019**, *78*, 1014–1029. [[CrossRef](#)] [[PubMed](#)]
- Valentin, N. Trends on biological deterioration of rocks and monumental stones. In *Congrès International sur la Conservation de la Pierre et Autres Matériaux*; UNESCO: Paris, France, 1993; pp. 30–34.
- Warscheid, T.; Braams, J. Biodeterioration of stone: A review. *Int. Biodeterior. Biodegrad.* **2000**, *46*, 343–368. [[CrossRef](#)]

10. Ciferri, O. The role of microorganisms in the degradation of cultural heritage. *Stud. Conserv.* **2002**, *47*, 35–45. [[CrossRef](#)]
11. Crispim, C.; Gaylarde, C. Cyanobacteria and Biodeterioration of Cultural Heritage: A Review. *Microb. Ecol.* **2005**, *49*, 1–9. [[CrossRef](#)] [[PubMed](#)]
12. Zhang, G.; Gong, C.; Gu, J.; Katayama, Y.; Someya, T.; Gu, J.D. Biochemical reactions and mechanisms involved in the biodeterioration of stone world cultural heritage under the tropical climate conditions. *Int. Biodeterior. Biodegrad.* **2019**, *143*, 104723. [[CrossRef](#)]
13. Favero-Longo, S.E.; Vannini, A.; Benesperi, R.; Bianchi, E.; Fačková, Z.; Giordani, P.; Malaspina, P.; Martire, L.; Matteucci, E.; Paoli, L.; et al. The application protocol impacts the effectiveness of biocides against lichens. *Int. Biodeterior. Biodegrad.* **2020**, *155*, 105105. [[CrossRef](#)]
14. Demoulin, T.; Girardet, F.; Flatt, R.J. Reprofiting of altered building sandstones: On-site measurement of the environmental conditions and their evolution in the stone. In *32èmes Rencontres de l'AUGC*; ETH: Zürich, Switzerland, 2014. [[CrossRef](#)]
15. Juhász, P.; Kopecskó, K.; Suhajda, Á. Analysis of capillary absorption properties of porous limestone material and its relation to the migration depth of bacteria in the absorbed biomineralizing compound. *Period. Polytech. Civ. Eng.* **2014**, *58*, 113–120. [[CrossRef](#)]
16. Monte, M. The influence of environmental conditions on the reproduction and distribution of epilithic lichens. *Aerobiologia* **1993**, *9*, 169–179. [[CrossRef](#)]
17. Ortega-Calvo, J.J.; Ariño, X.; Hernandez-Marine, M.; Saiz-Jimenez, C. Factors affecting the weathering and colonization of monuments by phototrophic microorganisms. *Sci. Total Environ.* **1995**, *167*, 329–341. [[CrossRef](#)]
18. Pinna, D. Microbial growth and its effects on inorganic heritage materials. In *Microorganisms in the Deterioration and Preservation of Cultural Heritage*; Joseph, E., Ed.; Springer: Berlin/Heidelberg, Germany, 2021; pp. 3–36.
19. Darlington, A. *Ecology of Walls*; Heinemann Educational Publishers: Portsmouth, NH, USA, 1981.
20. Chung, Y.J.; Seo, M.S.; Lee, K.S.; Han, S.H. The biodeterioration and conservation of stone historical monuments. *Conserv. Sci. Res.* **2003**, *5*–28.
21. Allsopp, D.; Seal, K.J.; Gaylarde, C.C. *Introduction to Biodeterioration*; Cambridge University Press: Cambridge, UK, 2004.
22. Jeong, S.H.; Lee, H.J.; Kim, D.W.; Chung, Y.J. New biocide for eco-friendly biofilm removal on outdoor stone monuments. *Int. Biodeterior. Biodegrad.* **2018**, *131*, 19–28. [[CrossRef](#)]
23. Kakakhel, M.A.; Wu, F.; Gu, J.D.; Feng, H.; Shah, K.; Wang, W. Controlling biodeterioration of cultural heritage objects with biocides: A review. *Int. Biodeterior. Biodegrad.* **2019**, *143*, 104721. [[CrossRef](#)]
24. Scheerer, S. *Microbial Biodeterioration of Outdoor Stone Monuments: Assessment Methods and Control Strategies*; Cardiff University: Cardiff, UK, 2008.
25. Cappitelli, F.; Cattò, C.; Villa, F. The control of cultural heritage microbial deterioration. *Microorganisms* **2020**, *8*, 1542. [[CrossRef](#)] [[PubMed](#)]
26. Caneva, G.; Nugari, M.P.; Pinna, D.; Salvadori, O. *Il Controllo del Degrado Biologico: I Biocidi nel Restauro dei Materiali Lapidari*; Nardini Editore: Fiesole, Italy, 1996; p. 151.
27. Nugari, M.P.; Salvadori, O. Biodeterioration control of cultural heritage: Methods and products. In *Molecular Biology and Cultural Heritage*; Saiz-Jimenez, C., Ed.; Routledge: London, UK, 2017; pp. 233–242.
28. Pinna, D. *Coping with Biological Growth on Stone Heritage Objects: Methods, Products, Applications, and Perspectives*; Apple Academic Press: Waretown, NJ, USA, 2017.
29. Russell, A.D.; Chopra, I. *Understanding Antibacterial Action and Resistance*; Ellis Horwood: London, UK, 1996; Volume 107.
30. Ghosh, S.K. Functional coatings and microencapsulation: A general perspective. In *Functional Coatings: By Polymer Microencapsulation*; Wiley: Hoboken, NJ, USA, 2006; pp. 1–28. [[CrossRef](#)]
31. Tiano, P. Biodeterioration of monumental rocks: Decay mechanisms and control methods. *Sci. Technol. Cult. Herit.* **1998**, *7*, 19–38.
32. Casanova Municchia, A.; Fidanza, M.R.; Caneva, G. Advances in testing the interference of biocides on stone materials: A comparative analysis and guidelines for a standardized approach. *J. Cult. Herit.* **2023**, *64*, 23–41. [[CrossRef](#)]
33. Liu, X.; Qian, Y.; Wang, Y.; Wu, F.; Wang, W.; Gu, J.D. Innovative approaches for the processes involved in microbial biodeterioration of cultural heritage materials. *Curr. Opin. Biotechnol.* **2022**, *75*, 102716. [[CrossRef](#)]
34. Fidanza, M.R.; Caneva, G. Natural biocides for the conservation of stone cultural heritage: A review. *J. Cult. Herit.* **2019**, *38*, 271–286. [[CrossRef](#)]
35. Villar-dePablo, M.; Ascaso, C.; Rodríguez-Pérez, E.; Urizal, M.; Wierzechos, J.; Pérez-Ortega, S.; de Los Ríos, A. Innovative approaches to accurately assess the effectiveness of biocide-based treatments to fight biodeterioration of Cultural Heritage monuments. *Sci. Total Environ.* **2023**, *897*, 165318. [[CrossRef](#)]
36. Varona, S.; Martín, Á.; Cocero, M.J. Formulation of a natural biocide based on lavandin essential oil by emulsification using modified starches. *Chem. Eng. Process. Process Intensif.* **2009**, *48*, 1121–1128. [[CrossRef](#)]
37. Fonseca, A.J.; Pina, F.; Macedo, M.F.; Leal, N.; Romanowska-Deskins, A.; Laiz, L.; Gómez-Bolea, A.; Saiz-Jimenez, C. Anatase as an alternative application for preventing biodeterioration of mortars: Evaluation and comparison with other biocides. *Int. Biodeterior. Biodegrad.* **2010**, *64*, 388–396. [[CrossRef](#)]
38. Palla, F.; Bruno, M.; Mercurio, F.; Tantillo, A.; Rotolo, V. Essential oils as natural biocides in the conservation of cultural heritage. *Molecules* **2020**, *25*, 730. [[CrossRef](#)] [[PubMed](#)]

39. Kaur, V.; Kaur, R.; Bhardwaj, U. A review on dill essential oil and its chief compounds as a natural biocide. *Flavour Fragr. J.* **2021**, *36*, 412–431. [[CrossRef](#)]
40. Pawłowska, A.; Stepczyńska, M. Natural biocidal compounds of plant origin as biodegradable materials modifiers. *J. Polym. Environ.* **2021**, *30*, 1683–1708. [[CrossRef](#)]
41. Gabriele, F.; Ranaldi, R.; Bruno, L.; Casieri, C.; Rugnini, L.; Spreti, N. Biodeterioration of stone monuments: Studies on the influence of bioreceptivity on cyanobacterial biofilm growth and on the biocidal efficacy of essential oils in natural hydrogel. *Sci. Total Environ.* **2023**, *870*, 161901. [[CrossRef](#)]
42. Spada, M.; Cuzman, O.A.; Tosini, I.; Galeotti, M.; Sorella, F. Essential oils mixtures as an eco-friendly biocidal solution for a marble statue restoration. *Int. Biodeterior. Biodegrad.* **2021**, *163*, 105280. [[CrossRef](#)]
43. Sasso, S.; Scrano, L.; Ventrella, E.; Bonomo, M.G.; Crescenzi, A.; Salzano, G.; Bufo, S.A. Natural biocides to prevent the microbial growth on cultural heritage. *Built Herit.* **2013**, *1*, 1035–1042.
44. Rotolo, V.; Barresi, G.; Di Carlo, E.; Giordano, A.; Lombardo, G.; Crimi, E.; Costa, E.; Bruno, M.; Palla, F. Plant extracts as green potential strategies to control the biodeterioration of cultural heritage. *Int. J. Conserv. Sci.* **2016**, *7*, 839–846.
45. Veneranda, M.; Blanco-Zubiaguirre, L.; Roselli, G.; Di Girolami, G.; Castro, K.; Madariaga, J.M. Evaluating the exploitability of several essential oils constituents as a novel biological treatment against cultural heritage biocolonization. *Microchem. J.* **2018**, *138*, 1–6. [[CrossRef](#)]
46. Argyri, A.A.; Doulgeraki, A.I.; Varla, E.G.; Bikouli, V.C.; Natskoulis, P.I.; Haroutounian, S.A.; Moulas, G.A.; Tassou, C.C.; Chorianopoulos, N.G. Evaluation of plant origin essential oils as herbal biocides for the protection of caves belonging to natural and cultural heritage sites. *Microorganisms* **2021**, *9*, 1836. [[CrossRef](#)]
47. Cattò, C.; Dell’Orto, S.; Villa, F.; Villa, S.; Gelain, A.; Vitali, A.; Marzano, V.; Baroni, S.; Forlani, F.; Cappitelli, F. Unravelling the structural and molecular basis responsible for the anti-biofilm activity of zosteric acid. *PLoS ONE* **2015**, *10*, e0131519. [[CrossRef](#)]
48. Md Zain, W.S.; Hairul Salleh, N.I.; Abdullah, A. Natural Biocides for Mitigation of Sulphate Reducing Bacteria. *Int. J. Corros.* **2018**, *2018*, 3567569. [[CrossRef](#)]
49. Borrego, S.; Valdés, O.; Vivar, I.; Lavin, P.; Guiamet, P.; Battistoni, P.; Gómez de Saravia, S.; Borges, P. Essential Oils of Plants as Biocides against Microorganisms Isolated from Cuban and Argentine Documentary Heritage. *ISRN Microbiol.* **2012**, 826786. [[CrossRef](#)]
50. Stupar, M.; Grbic, M.; Džamić, A.M.; Unković, N.; Ristić, M.S.; Jelikić, A.; Vukojevic, J. Antifungal activity of selected essential oils and biocide benzalkonium chloride against the fungi isolated from cultural heritage objects. *S. Afr. J. Bot.* **2014**, *93*, 118–124. [[CrossRef](#)]
51. Elsayed, Y.; Shabana, Y. The effect of some essential oils on aspergillus niger and alternaria alternata infestation in archaeological oil paintings. *Mediterr. Archaeol. Archaeom.* **2018**, *18*, 71–87. [[CrossRef](#)]
52. Macedo-Arantes, S.; Piçarra, A.; Caldeira, A.T.; Candeias, A.E.; Martins, M.R. Essential oils of Portuguese flavouring plants: Potential as green biocides in cultural heritage. *Eur. Phys. J. Plus* **2021**, *136*, 1106. [[CrossRef](#)]
53. Maia, F.; Silva, A.P.; Fernandes, S.; Cunha, A.; Almeida, A.; Tedim, J.; Zheludkevich, M.L.; Ferreira, M.G.S. Incorporation of biocides in nanocapsules for protective coatings used in maritime applications. *Chem. Eng. J.* **2015**, *270*, 150–157. [[CrossRef](#)]
54. Dresler, C.; Saladino, M.L.; Demirbag, C.; Caponetti, E.; Martino, D.F.C.; Alduina, R. Development of controlled release systems of biocides for the conservation of cultural heritage. *Int. Biodeterior. Biodegrad.* **2017**, *125*, 150–156. [[CrossRef](#)]
55. Ruggiero, L.; Di Bartolomeo, E.; Gasperi, T.; Luisetto, I.; Talone, A.; Zurlo, F.; Peddis, D.; Ricci, M.A.; Sodo, A. Silica nanosystems for active antifouling protection: Nanocapsules and mesoporous nanoparticles in controlled release applications. *J. Alloys Compd.* **2019**, *798*, 144–148. [[CrossRef](#)]
56. Ruggiero, L.; Bartoli, F.; Fidanza, M.R.; Zurlo, F.; Marconi, E.; Gasperi, T.; Tuti, S.; Crociani, L.; Di Bartolomeo, E.; Caneva, G.; et al. Encapsulation of environmentally-friendly biocides in silica nanosystems for multifunctional coatings. *Appl. Surf. Sci.* **2020**, *514*, 145908. [[CrossRef](#)]
57. Marconi, E.; Luisetto, I.; Di Carlo, G. 3-APTES on Dendritic Fibrous Mesoporous Silica Nanoparticles for the pH-Controlled Release of Corrosion Inhibitors. *Nanomaterials* **2023**, *13*, 2543. [[CrossRef](#)] [[PubMed](#)]
58. Jämsä, S.; Mahlberg, R.; Holopainen, U.; Ropponen, J.; Savolainen, A.; Ritschkoff, A.C. Slow release of a biocidal agent from polymeric microcapsules for preventing biodeterioration. *Prog. Org. Coat.* **2013**, *76*, 269–276. [[CrossRef](#)]
59. Presentato, A.; Armetta, F.; Spinella, A.; Chillura Martino, D.F.; Alduina, R.; Saladino, M.L. Formulation of Mesoporous Silica Nanoparticles for Controlled Release of Antimicrobials for Stone Preventive Conservation. *Front. Chem.* **2020**, *8*, 699. [[CrossRef](#)]
60. Bartoli, F.; Zuenä, M.; Sodo, A.; Caneva, G. The Efficiency of Biocidal Silica Nanosystems for the Conservation of Stone Monuments: Comparative In Vitro Tests against Epilithic Green Algae. *Appl. Sci.* **2021**, *11*, 6804. [[CrossRef](#)]
61. Heiden, P.; Matuana, L.; Dawson-Andoh, B. *Nanotechnology: A Novel Approach to Prevent Biocide Leaching*; US EPA Archive Document. 2016. Available online: <https://archive.epa.gov/ncer/publications/web/html/heiden.html> (accessed on 20 October 2023).
62. Caldeira, A.T. Green mitigation strategy for cultural heritage using bacterial biocides. In *Microorganisms in the Deterioration and Pre Servation of Cultural Heritage*; Springer: Berlin/Heidelberg, Germany, 2021; p. 137.
63. Franco-Castillo, I.; Hierro, L.; de la Fuente, J.M.; Seral-Ascaso, A.; Mitchell, S.G. Perspectives for antimicrobial nanomaterials in cultural heritage conservation. *Chem* **2021**, *7*, 629–669. [[CrossRef](#)]
64. Gomez-Villalba, L.S.; Salcines, C.; Fort, R. Application of Inorganic Nanomaterials in Cultural Heritage Conservation, Risk of Toxicity, and Preventive Measures. *Nanomaterials* **2023**, *13*, 1454. [[CrossRef](#)] [[PubMed](#)]

65. Geiger, T.; Delavy, P.; Hany, R.; Schleuniger, J.; Zinn, M. Encapsulated zosteric acid embedded in poly [3-hydroxyalkanoate] coatings—Protection against biofouling. *Polym. Bull.* **2004**, *52*, 65–72. [[CrossRef](#)]
66. Villa, F.; Albanese, D.; Giussani, B.; Stewart, P.S.; Daffonchio, D.; Cappitelli, F. Hindering biofilm formation with zosteric acid. *Biofouling* **2010**, *26*, 739–752. [[CrossRef](#)]
67. Villa, F.; Pitts, B.; Stewart, P.S.; Giussani, B.; Roncoroni, S.; Albanese, D.; Giordano, C.; Tunesi, M.; Cappitelli, F. Efficacy of zosteric acid sodium salt on the yeast biofilm model *Candida albicans*. *Microb. Ecol.* **2011**, *62*, 584–598. [[CrossRef](#)] [[PubMed](#)]
68. Vilas-Boas, C.; Sousa, E.; Pinto, M.; Correia-da-Silva, M. An antifouling model from the sea: A review of 25 years of zosteric acid studies. *Biofouling* **2017**, *33*, 927–942. [[CrossRef](#)] [[PubMed](#)]
69. Xu, Q.; Barrios, C.A.; Cutright, T.; Zhang Newby, B.M. Evaluation of toxicity of capsaicin and zosteric acid and their potential application as antifoulants. *Environ. Toxicol. Int. J.* **2005**, *20*, 467–474. [[CrossRef](#)] [[PubMed](#)]
70. Franchini, C.; Muraglia, M.; Corbo, F.; Florio, M.A.; Di Mola, A.; Rosato, A.; Matucci, R.; Nesi, M.; Van Bambeke, F.; Vitali, C. Synthesis and biological evaluation of 2-mercapto-1, 3-benzothiazole derivatives with potential antimicrobial activity. *Arch. Pharm. Int. J. Pharm. Med. Chem.* **2009**, *342*, 605–613. [[CrossRef](#)] [[PubMed](#)]
71. Zuena, M.; Ruggiero, L.; Della Ventura, G.; Bemporad, E.; Ricci, M.A.; Sodo, A. Effectiveness and compatibility of nanoparticle based multifunctional coatings on natural and man-made stones. *Coatings* **2021**, *11*, 480. [[CrossRef](#)]
72. Haake, S.; Simon, S.; Favaro, M. The bologna cocktail-evaluation of consolidation treatments on monuments in France and Italy after 20 years on natural aging. In Proceedings of the 10th International Congress on Deterioration and Conservation of Stone, Stockholm, Sweden, 27 June–2 July 2004; pp. 423–430.
73. Commissione Beni Culturali Uni Normal. *Normal 43/93 Misure Colorimetriche di Superfici Opache (Italian Normative on Stone Material-Colorimetric Measurement of Opaque Surfaces)*; Commissione Beni Culturali Uni Normal: Roma, Italy, 1993.
74. Zuena, M.; Ruggiero, L.; Caneva, G.; Bartoli, F.; Ventura, G.D.; Ricci, M.A.; Sodo, A. Assessment of Stone Protective Coatings with a Novel Eco-Friendly Encapsulated Biocide. *Coatings* **2021**, *11*, 1109. [[CrossRef](#)]
75. ASTM D4303-10; Standard Test Methods for Lightfastness of Colorants Used In Artists' Materials. ASTM International: West Conshohocken, PA, USA, 2010.
76. UNI-EN-15886; Misura del Colore Delle Superfici ICS: 97.195. Conservazione dei Beni Culturali 2010. 2010.
77. Bartoli, F.; Mucicchia, A.C.; Leotta, M.; Luciano, S.; Caneva, G. Biological recolonization dynamics: Kentridge's artwork disappearing along the Tiber embankments (Rome, Italy). *Int. Biodeterior. Biodegrad.* **2021**, *160*, 105214. [[CrossRef](#)]
78. Rubio, F.; Rubio, J.; Oteo, J.L. FT-IR Study of the Hydrolysis of Tetraethylorthosilicate (TEOS), Spectroscopy Letters. *Int. J. Rapid Commun.* **1998**, *31*, 199–219. [[CrossRef](#)]
79. Ruggiero, L.; Fidanza, M.R.; Iorio, M.; Tortora, L.; Caneva, G.; Ricci, M.A.; Sodo, A. Synthesis and characterization of TEOS coating added with innovative antifouling silica nanocontainers and TiO₂ nanoparticles. *Front. Mater.* **2020**, *7*, 185. [[CrossRef](#)]
80. Quagliarini, E.; Bondioli, F.; Goffredo, G.B.; Licciulli, A.; Munafo, P. Smart surfaces for architectural heritage: Preliminary results about the application of TiO₂-based coatings on travertine. *J. Cult. Herit.* **2012**, *13*, 204–209. [[CrossRef](#)]
81. Wibowo, D.; Hue, Y.; Middelberg, A.P.J.; Zhao, C.-X. Interfacial engineering for silica nanocapsules. *Adv. Colloid Interface Sci.* **2016**, *236*, 83–100. [[CrossRef](#)]
82. Haynie, F.H. Deterioration of marble. *Durab. Build. Mater.* **1983**, *1*, 241–254.
83. Wang, H.-P.; Fei, W.; Ngothai, Y.; O'Neill, B. A kinetic model of the 'Fe²⁺ oxidisation' process for colour enhancement in natural marble. *Mater. Chem. Phys.* **2004**, *86*, 51–58. [[CrossRef](#)]
84. Wolfaardt, G.M.; Cloete, T.E. The effect of some environmental parameters on surface colonization by microorganisms. *Water Res.* **1992**, *26*, 527–537. [[CrossRef](#)]
85. Tomaselli, L.; Lamenti, G.; Bosco, M.; Tiano, P. Biodiversity of photosynthetic micro-organisms dwelling on stone monuments. *Int. Biodeterior. Biodegrad.* **2000**, *46*, 251–258. [[CrossRef](#)]
86. Macedo, M.F.; Miller, A.Z.; Dionísio, A.; Saiz-Jimenez, C. Biodiversity of cyanobacteria and green algae on monuments in the Mediterranean Basin: An overview. *Microbiology* **2009**, *11*, 3476–3490. [[CrossRef](#)] [[PubMed](#)]
87. Aung, K.; Jiang, Y.; He, Y.S. The role of water in plant-microbe interactions. *Plant J.* **2018**, *93*, 771–780. [[CrossRef](#)] [[PubMed](#)]
88. Louati, M.; Ennis, N.J.; Ghodhbane-Gtari, F.; Hezbri, K.; Sevigny, J.L.; Fahnestock, M.F.; Cherif-Silini, H.; Bryce, J.G.; Tisa, L.S.; Gtari, M. Elucidating the ecological networks in stone-dwelling microbiomes. *Environ. Microbiol.* **2020**, *22*, 1467–1480. [[CrossRef](#)] [[PubMed](#)]
89. Yarwood, R.; Rockhold, M.; Niemet, M.R.; Selker, J.S.; Bottomley, P.J. Impact of microbial growth on water flow and solute transport in unsaturated porous media. *Water Resour. Res.* **2006**, *42*, 1–11. [[CrossRef](#)]
90. Kapridaki, C.; Maravelaki-Kalaitzaki, P. TiO₂-SiO₂-PDMS nano-composite hydrophobic coating with self-cleaning properties for marble protection. *Prog. Org. Coat.* **2013**, *76*, 400–410. [[CrossRef](#)]
91. Adamopoulos, F.G.; Vouvoudi, E.C.; Pavlidou, E.; Achilias, D.S.; Karapanagiotis, I. TEOS-Based Superhydrophobic Coating for the Protection of Stone-Built Cultural Heritage. *Coatings* **2021**, *11*, 135. [[CrossRef](#)]
92. Bellinzoni, A.M.; Caneva, G.; Ricci, S. Ecological trends in travertine colonisation by pioneer algae and plant communities. *Int. Biodeterior. Biodegrad.* **2003**, *51*, 203–210. [[CrossRef](#)]
93. Gaylarde, C. Influence of environment on microbial colonization of historic stone buildings with emphasis on cyanobacteria. *Heritage* **2020**, *3*, 1469–1482. [[CrossRef](#)]

94. Bartoli, F.; Isola, D.; Casanova Municchia, A.; Kumbaric, A.; Caneva, G. Science for art: Multi-years' evaluations of biocidal efficacy in support of artwork conservation. *Front. Microbiol.* **2023**, *14*, 1178900. [[CrossRef](#)] [[PubMed](#)]
95. Caneva, G.; Bartoli, F.; Savo, V.; Futagami, Y.; Strona, G. Combining Statistical Tools and Ecological Assessments in the Study of Biodeterioration Patterns of Stone Temples in Angkor (Cambodia). *Sci. Rep.* **2016**, *6*, 32601. [[CrossRef](#)] [[PubMed](#)]
96. Caneva, G.; Bartoli, F.; Ceschin, S.; Salvadori, O.; Futagami, Y.; Salvati, L. Exploring ecological relationships in the biodeterioration patterns of Angkor temples (Cambodia) along a forest canopy gradient. *J. Cult. Herit.* **2015**, *16*, 728–735. [[CrossRef](#)]
97. Odum, E.P.; Barrett, G.W. *Fundamentals of Ecology*; Saunders: Philadelphia, PA, USA, 1971; Volume 3, p. 5.
98. Achamlale, S.; Rezzonico, B.; Grignon-Dubois, M. Evaluation of *Zostera detritus* as a potential new source of zosteric acid. *J. Appl. Phycol.* **2009**, *21*, 347–352. [[CrossRef](#)]
99. Newby, B.M.Z.; Cutright, T.; Barrios, C.A.; Xu, Q. Zosteric acid—An effective antifoulant for reducing freshwater bacterial attachment on coatings. *JCT Res.* **2006**, *3*, 69–76. [[CrossRef](#)]

Disclaimer/Publisher's Note: The statements, opinions and data contained in all publications are solely those of the individual author(s) and contributor(s) and not of MDPI and/or the editor(s). MDPI and/or the editor(s) disclaim responsibility for any injury to people or property resulting from any ideas, methods, instructions or products referred to in the content.